



ELSEVIER

Journal of Chromatography A, 797 (1998) 93–102

JOURNAL OF
CHROMATOGRAPHY A

Comparative studies of structural and surface properties of porous inorganic oxides used in liquid chromatography

C.P. Jaroniec, M. Jaroniec*, M. Kruk

Department of Chemistry, Kent State University, Kent, OH 44242, USA

Abstract

Structural and surface properties of chromatographic porous silica, alumina, titania and zirconia were studied using thermogravimetry and nitrogen adsorption. The samples studied are mesoporous and exhibit relatively narrow pore size distributions in the range from 10 to 30 nm, making them suitable for chromatographic applications. Low-pressure nitrogen adsorption and thermogravimetry were used to monitor the effects of the thermal treatment on the surface properties of the samples. The observed changes in surface properties caused by treatments at different temperatures were explained in terms of the desorption of physically/chemically adsorbed water, which led to exposure of high energy adsorption sites. © 1998 Elsevier Science B.V.

Keywords: Stationary phases, LC; Packing materials; Inorganic oxide packing materials

1. Introduction

Native and surface-modified porous inorganic oxides, such as silica, alumina, zirconia and titania, are used as chromatographic packings. Among these, silica-based chemically bonded phases are the most commonly used in analytical and preparative separations under hydro-organic conditions [1]. The popularity of silica-based packings can be attributed to the relative ease with which the surface properties of these materials can be tailored [1,2], providing mechanically, thermally and chemically stable bonded phases with specific surface properties [3]. However, the use of silica-based chromatographic packings is usually limited to the pH range of about 2 to 8. This pH range can be extended to 11 when the double-encapped silica-based bonded phases are used with organic buffers below 313 K [4]. At low pH, the chemically bonded ligands are slowly re-

moved from the surface via the hydrolysis of siloxane linkages [5,6] and at high pH values, the dissolution of the silica matrix takes place [7,8]. Due to the low stability of silica-based materials at low and high pH values, other porous inorganic oxides, e.g., alumina, zirconia and titania, which are significantly more stable under these conditions, are becoming popular as chromatographic packings [9–12]. While stable analogs of silica-based chemically bonded phases are difficult to prepare using alumina, zirconia and titania, these porous oxides can be modified by various alternative methods and used as chromatographic packings under hydro-organic conditions [10,12].

Column packing materials for high-performance liquid chromatography (HPLC) need to fulfil certain requirements. A good chromatographic packing should have high mechanical, thermal and chemical stability, a relatively high surface area, and its surface and structural properties should be easy to modify. Moreover, processes for preparing materials

*Corresponding author.

of desired particle size, shape and pore size in a reproducible fashion should be well-established. Chromatographic silica and silica-based bonded phases meet all of the above criteria, with the exception of chemical stability at high and low pH. As a result, HPLC-grade silica is commercially available in a variety of particle sizes, shapes and pore sizes, and is extensively used in chromatographic applications. On the other hand, the processes for the preparation of chromatographic grade inorganic oxides other than silica are not as well-established, and chromatographic grade alumina, zirconia and titania are commercially available from a limited number of vendors [12,13]. It should be noted here that the porous inorganic oxides studied in the current work are ones, which are commercially available and used in chromatographic applications.

Chromatographic properties of packing materials are influenced not only by size and shape of their particles, but also by their surface and porous properties. The latter can be evaluated by nitrogen adsorption at 77 K and high resolution thermogravimetry (TGA), and their assessment facilitates the chromatographic applications of unmodified and physically and/or chemically modified inorganic oxides. Nitrogen adsorption at 77 K has been used in extensive studies of chromatographic packings including unmodified [14–16], chemically modified [16–18] and physically coated [17] silica gels.

Nitrogen adsorption has been traditionally used for the estimation of the specific surface area and the pore size distribution [19] of chromatographic packings. However, adsorption measurements can also be used to evaluate the energetic heterogeneity of these materials, where the calculation of the adsorption energy distribution (AED) functions [20] is especially important and interesting. The AED function is assessed from low-pressure adsorption data and describes the interaction of nitrogen probe molecules with sites of different adsorption energies present on the surface of the material studied. These functions can be used in a comparative fashion [16–18] to evaluate the changes in the properties of materials induced by the surface modification, e.g., the introduction or removal of high energy adsorption sites. It must be realized that the adsorption energy is defined for an adsorbent–adsorbate system. Therefore, the use of nitrogen molecules to probe the surface of

porous inorganic oxides can be expected to provide the most basic information about the oxide surfaces, because nitrogen interacts with these surfaces via nonspecific, dispersive interactions. Consequently, if differences in the energies of adsorption sites are observed for nitrogen, it is likely that these differences will be even more pronounced for adsorbate molecules which exhibit specific interactions (e.g., hydrogen bonding) with these surfaces.

Thermogravimetry can be used to evaluate the thermal stability of inorganic oxides and the interaction of their surfaces with various probe molecules, e.g., water, alcohols and hydrocarbons. TGA has been used to study unmodified silica [21–23], chemically modified and physically coated silica [18,24], alumina [25] and zirconia [26]. The results of TGA measurements can supplement the adsorption characterization of porous inorganic oxides in order to provide a thorough understanding of their surface and structural properties, which facilitates the applications of these materials as chromatographic packings.

2. Experimental

2.1. Materials

LiChrospher Si-100 silica, Aluspher AL100 alumina, PICA-7 zirconia, 100A titania were obtained from EM Science (Gibbstown, NJ, USA), E. Merck (Darmstadt, Germany), Zirchrom Separations (Anoka, MN, USA) and YMC (Wilmington, NC, USA), respectively. LiChrospher Si-100 silica and Aluspher AL 100 are amorphous samples, whereas PICA-7 zirconia and 100A titania possess a crystalline bulk structure (see details in Ref. [12]).

2.2. Characterization methods

Nitrogen adsorption–desorption isotherms at 77 K were measured in the relative pressure range of 10^{-6} to 0.99 on a Micromeritics model ASAP 2010 (Norcross, GA, USA) adsorption analyzer. Pre-purified grade nitrogen was used. Prior to the analysis, the inorganic oxide samples were outgassed for 2

h, with the exception of the alumina samples which were outgassed for 4 h, in the degas port of the adsorption apparatus at various temperatures in the 373–623 K range under vacuum of about 10^{-3} Torr (1 Torr=133.322 Pa). The high resolution thermogravimetric measurements were carried out using a TA Instruments model TA 2950 (New Castle, DE, USA) thermogravimetric analyzer. The oxides were heated in a dry nitrogen atmosphere from ambient temperature up to 1273 K using a heating rate of 5 K/min.

2.3. Calculation methods

The specific surface areas S_{BET} of the inorganic oxides studied were calculated using the standard Brunauer–Emmett–Teller (BET) method [27] from adsorption data in the relative pressure (p/p_0) range of 0.06 to 0.25, where p and p_0 denote the equilibrium and saturation pressures of nitrogen at 77 K, respectively. The total pore volumes V_t were evaluated by converting the volume of adsorbed nitrogen at p/p_0 of approximately 0.98 to the volume of liquid adsorbate. The pore size distributions for the oxides were evaluated from the desorption data using the Barrett–Joyner–Halenda (BJH) method [28]. The BJH method uses the Kelvin equation with a correction for the statistical film thickness on the pore walls to relate the capillary evaporation pressure with the pore size. Moreover, it takes into account the decrease of the statistical film thickness in pores, which were already emptied during the desorption process. The BJH method is expected to provide a reasonable pore size evaluation for the inorganic oxides studied, since their mesopores have sizes significantly above an estimated lower limit of the validity of the Kelvin equation [29]. Note that according to the IUPAC recommendations [30,31] the pores are classified as micropores (widths below 2 nm), mesopores (widths between 2 and 50 nm) and macropores (widths above 50 nm).

The adsorption energy distribution functions for the inorganic oxides studied were calculated from submonolayer adsorption data (i.e. $v < v^0$, where v is the volume adsorbed and v^0 is the BET monolayer capacity) by inverting the integral equation of adsorption [20]:

$$\Theta(p) = \int_{\epsilon_{\min}}^{\epsilon_{\max}} \theta(p, \epsilon) F(\epsilon) d\epsilon \quad (1)$$

where $\Theta(p)$ is the total relative adsorption defined as the ratio of the volume adsorbed to the BET monolayer capacity and ϵ is the adsorption energy in the interval from ϵ_{\min} to ϵ_{\max} . $\theta(p, \epsilon)$ is the local adsorption isotherm as a function of the adsorption energy and $F(\epsilon)d\epsilon$ is the fraction of the surface sites with adsorption energies between ϵ and $\epsilon+d\epsilon$. The Fowler–Guggenheim (FG) equation [20,32], which describes localized monolayer adsorption with lateral interactions on adsorption sites of energy ϵ , was assumed to represent the local adsorption isotherm:

$$\theta(p, \epsilon) = \frac{Kp \exp(z\omega\theta/k_B T)}{1 + Kp \exp(z\omega\theta/k_B T)} \quad (2)$$

where K is the Langmuir constant for adsorption on monoenergetic sites, z is the number of nearest neighbors of an adsorbate molecule in the monolayer, ω is the interaction energy between a pair of nearest neighbors, k_B is the Boltzmann constant and T is the absolute temperature. The Langmuir constant K is defined as

$$K = K_0(T) e^{\epsilon/k_B T} \quad (3)$$

where $K_0(T)$ is the pre-exponential factor, which can be expressed in terms of the partition functions for an isolated adsorbate molecule in the gas and surface phases [20,32]. The form of the FG equation used [Eq. (2)] implies a random distribution of adsorption sites, which appears to be a realistic model for the surfaces of porous inorganic oxides due to their noncrystallinity and the presence of various surface groups [16]. The AED functions for the oxides studied were calculated using the INTEG program which uses the regularization method [33] to invert the integral equation of adsorption [Eq. (1)] with respect to $F(\epsilon)$. The interaction parameters $z=4$, $\omega/k_B=95$ K and the regularization parameter $\gamma=0.1$ were assumed in all calculations [15,16].

3. Results and discussion

Nitrogen adsorption isotherms for the chromatographic porous oxides are shown in Fig. 1. These

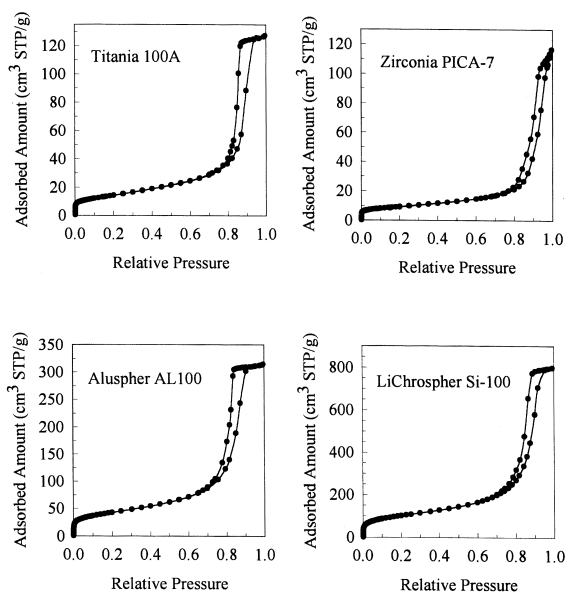


Fig. 1. Nitrogen adsorption isotherms for the chromatographic porous oxides.

isotherms were measured on samples outgassed at the lowest temperature from the series of measurements for each oxide, but the outgassing temperature significantly affects only the low-pressure parts of the isotherms which are not visible on the linear scale of Fig. 1. The uptake of nitrogen by the inorganic oxide samples proceeded as monolayer-multilayer adsorption followed by capillary condensation, i.e. instantaneous filling of mesopores with adsorbate, in the relative pressure range from ca. 0.7 to 0.8. Upon desorption, pronounced hysteresis was observed for all samples under study. The adsorption isotherms are of type IV according to the IUPAC recommendations [30,31]. This type of isotherm is characteristic for mesoporous samples which do not contain an appreciable amount of macropores. The hysteresis loop for zirconia is of type H1 and the loops for the remaining samples are intermediate between types H1 and H2 [30,31]. As is indicated by narrow hysteresis loops with steep and nearly parallel adsorption and desorption branches, the oxides studied appear to have good pore connectivity and relatively narrow pore size distributions. It was previously reported [10] that inorganic oxides,

which exhibit type IV adsorption isotherms with H1 hysteresis loops are the most suitable for chromatographic purposes.

The pore size distributions for the inorganic oxides, calculated from the desorption branches of isotherms using the BJH method [28], are shown in Fig. 2. The pore size distribution curves for titania, alumina and silica are relatively narrow and centered between 10 and 20 nm. The distribution curve for the zirconia sample appears to be bimodal (maxima in the pore size range from 10 to 25 nm), which is in agreement with the distribution obtained from mercury porosimetry for a zirconia sample prepared via the polymerization-induced colloid aggregation (PICA) method and sintered at about 1200 K [10]. As it was mentioned earlier, the narrow pore size distributions centered in the intermediate mesopore range are desirable for the applications of inorganic oxides as chromatographic packings.

Shown in Table 1 are the structural properties of the chromatographic porous oxides studied, which include the average particle size (provided by the manufacturers), total pore volume and average pore size. The total pore volumes of the inorganic oxides under study were not affected appreciably by the

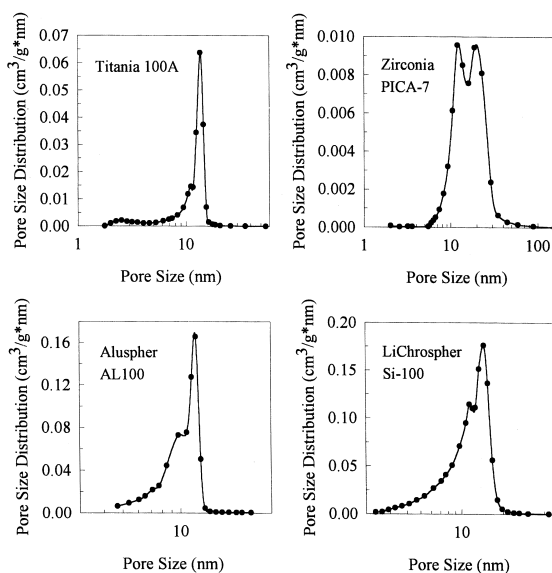


Fig. 2. Pore size distributions of the porous oxides calculated from desorption data using the Barrett–Joyner–Halenda method.

Table 1
Structural and surface properties of the chromatographic porous oxides under study

Sample	Average particle size (μm)	Average pore size (nm)	Total pore volume (cm^3/g)	Amount of adsorbed water ($\mu\text{mol}/\text{m}^2$) ^a
Titania 100A	5	12.5	0.20	22.1
Zirconia PICA-7	2.5	25.8	0.15	19.6
Aluspher AL100	5	10.7	0.50	29.7
LiChrospher Si-100	10	12.9	1.23	10.2

^a Amount of physically and/or chemically adsorbed water was estimated using TGA measurements from the mass-loss at 623 K.

temperature at which the material was outgassed (from 373 to 623 K). However, small systematic changes were observed in the BET specific surface areas of some of the oxide samples, as a result of the thermal treatment (see Table 2). For the silica, the BET specific surface area remained essentially the same after treatment at 413, 473 and 623 K. It should be noted here that in comparison with our previous studies [17,18], differences of about 6% were observed in both the specific surface area and total pore volume for LiChrospher Si-100 silica. However, the previously reported and currently measured adsorption isotherms have essentially identical shape and

are simply scaled by a factor of about 1.06. This can be attributed to the experimental error of the adsorption measurements performed under slightly different conditions, e.g., different sample tubes, different masses of the sample used, etc.. On the other hand, those types of errors are not expected to influence the results of comparative studies performed on the same sample in the same sample tube, as was the case in the current study. Moreover, it was observed that the thermal treatment for some samples led to a significant change of the overall shape of the low-pressure adsorption isotherms, and did not just systematically scale all adsorption data. So the changes induced by the thermal treatment reported in the current work are meaningful and do not arise simply from experimental errors.

Although the BET specific surface area for the silica was not dependent on the degassing temperatures in the 413–623 K range, systematic changes were observed between the titania, zirconia and alumina samples treated at different temperatures. For Titania 100A a difference of about 10% in the BET specific surface area was observed for samples outgassed at 373 and 623 K. The largest increases in S_{BET} occurred after treating the sample at 413 K and then at 473 K. Outgassing the titania sample at temperatures between 473 and 623 K had a much smaller effect on the BET surface area of the sample. The BET surface area of Zirconia PICA-7 slowly increased following the thermal treatment at temperatures in the 373–623 K range, where the difference for samples outgassed at 373 and 623 K was about 3%. The difference in the BET surface area for samples of Aluspher AL100 outgassed at 393 and 623 K was about 5%. It should be noted that for this

Table 2
Effect of the thermal treatment on the specific surface areas of the chromatographic porous oxides

Sample	Treatment temperature (K)	BET surface area (m^2/g)
Titania 100A	373	52
	413	55
	473	57
	573	58
	623	58
Aluspher AL100	393	152
	473	153
	623	160
Zirconia PICA-7	373	33
	413	33
	473	33
	623	34
LiChrospher Si-100	413	360
	473	360
	623	360

oxide, S_{BET} remained essentially unchanged after the treatment at 393 and 473 K, and the 5% increase in the BET specific surface area occurred following the treatment at 623 K.

Shown in Fig. 3 is the effect of the thermal treatment at temperatures between 373 and 623 K on the low-pressure adsorption behavior of the inorganic oxides studied. The adsorption energy distribution functions calculated using submonolayer adsorption data are shown in Fig. 4. No significant changes were observed in the low-pressure adsorption isotherm (Fig. 3) and the AED function (Fig. 4) for LiChrospher Si-100 treated at 413, 473 and 623 K. However, the thermal treatment induced significant changes in the low-pressure adsorption behavior for the remaining oxides, where the effect of the treatment was most pronounced for the Titania 100A sample. The low-pressure adsorption increased significantly for titania as the sample was treated at temperatures from 373 to 623 K, and the initial part of the isotherm (p/p_0 range from 10^{-6} to 10^{-4}) for the sample treated at 623 K is similar to isotherms measured for microporous adsorbents. Similar changes in the adsorption profiles appeared to be present, but to a much smaller extent, for zirconia and alumina samples treated at 623 K. However, it is

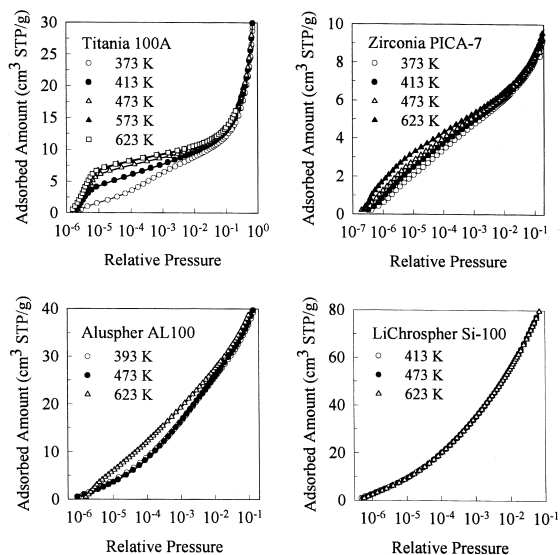


Fig. 3. Comparison of low-pressure nitrogen adsorption isotherms for the porous oxides thermally treated at different temperatures in the range from 373 to 623 K.

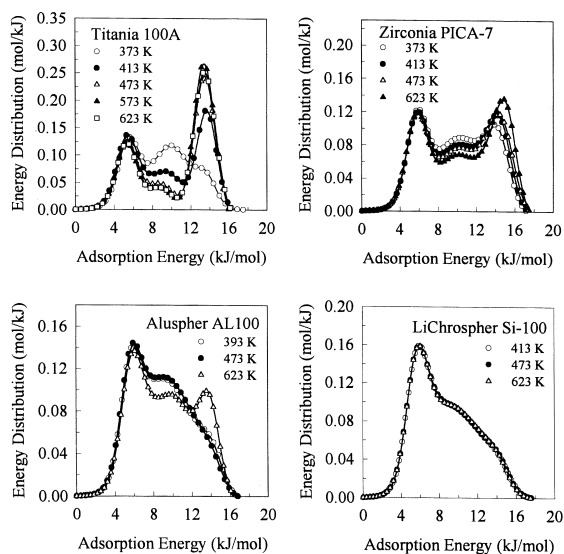


Fig. 4. Comparison of nitrogen adsorption energy distributions for the porous oxides thermally treated at different temperatures in the range from 373 to 623 K.

very unlikely that micropores were created by the thermal treatment, because the adsorption isotherms nearly converge at the relative pressure of about 0.1 for all oxide samples. Rather, it appears that the thermal treatment of the porous inorganic oxides removed adsorbed species from their surfaces (most likely physically and/or chemically adsorbed water), thereby exposing high energy adsorption sites which can strongly interact with the nitrogen probe molecules.

The above interpretation was supported by high resolution thermogravimetric measurements. The mass-loss (TGA) curves and the derivative mass-loss (DTG) curves for the porous inorganic oxides are shown in Fig. 5. Using the mass-losses at 623 K, the amounts of physically and/or chemically adsorbed water on the surfaces of the oxide samples, expressed as μmol of water per m^2 of dry oxide ($\mu\text{mol}/\text{m}^2$), could be estimated. It was assumed that it is only water that desorbs up to 623 K and that all surface coordinated water, physisorbed or chemisorbed excluding “permanent” hydroxyl groups (e.g., silanols or residual hydroxyl groups on titania) is removed up to 623 K. The examination of the TGA curves for the oxides indicates that the assumption that all physically/chemically adsorbed species

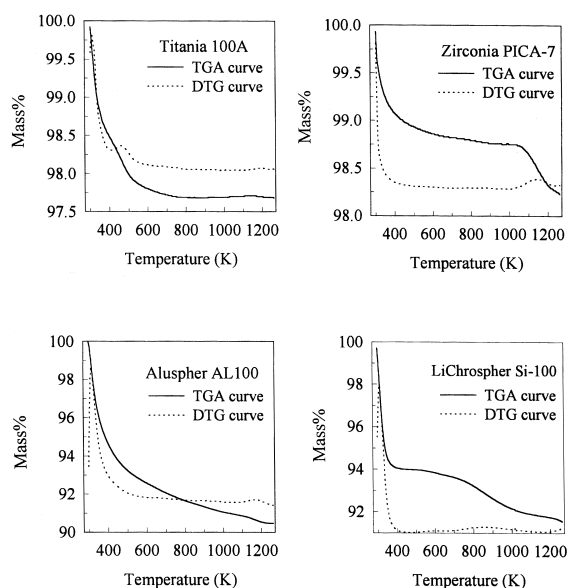


Fig. 5. Thermogravimetric weight-loss curves for the porous oxides under study.

are already removed at 623 K is quite reasonable for all samples, possibly with the exception of Aluspher AL100, for which the TGA curve does not level off at temperatures close to 623 K.

The Titania 100A material showed a significant mass-loss up to about 600 K, which can be attributed to the thermodesorption of different types of adsorbed water. Moreover, it appears that the titania surface possesses at least two main types of sites with respect to water adsorption, which can be seen from the two distinct maxima in its derivative mass-loss curve. The TGA curve for titania is relatively flat following the large mass-loss up to about 600 K and it can be assumed that at about 623 K the sample contains no significant amounts of water. It is interesting to note that on the basis of infra-red measurements [34,35], dry anatase was reported to possess two distinct types of residual hydroxyl groups, which are present even after evacuation at 973 K [34].

The Zirconia PICA-7 sample exhibits a significant mass-loss up to about 600 K and a much smaller further mass-loss up to about 1000 K. According to infrared measurements [37], porous zirconia loses physisorbed and coordinated water up to approximately 473 K. Between 473 and about 1200 K,

different types of chemisorbed water, including surface hydroxyl groups, are removed from the surface [26]. In the case of porous zirconia one should also be concerned with the strong adsorption of carbon dioxide onto the surface [37,38]. As previously reported on the basis of coupled TGA and mass spectroscopy [26], chemisorbed CO_2 is removed from the zirconia surface at temperatures between 673 and 973 K. Moreover, it was shown [26] that water vapor inhibits the adsorption of CO_2 on zirconia. For the particular zirconia sample under study, there does not appear to be a significant amount of chemisorbed carbon dioxide because a very small mass-loss is observed in the 600–1000 K range. The thermal treatment of the sample up to 623 K probably removes mostly physically adsorbed water (largest mass-loss takes place up to about 500 K) and some chemisorbed water between about 500 and 623 K. Moreover, if small amounts of adsorbed CO_2 are present, they would not be removed by the thermal treatment up to 623 K [26]. Therefore, any CO_2 will be present in equal amounts for all zirconia samples under study, and the thermodesorption of CO_2 should not be a factor in the changes observed in the low-pressure isotherms for zirconia (Fig. 3). On the basis of infrared measurements [10,39,40], zirconia with no significant amount of physically adsorbed water, has been reported to contain two easily distinguishable types of hydroxyl groups (i.e. single and bridged).

The Aluspher AL100 sample exhibits a continuous mass-loss up to about 1200 K. The largest decrease in the mass of the material (about 8%) takes place up to 600 K, but a significant mass-loss (about 2%) still occurs in the 600–1200 K region. It appears that the alumina sample contains various types of physically and chemically adsorbed water [41], which are gradually removed at different temperatures from 300 to 1200 K. Therefore, the use of mass-loss at 623 K to calculate the amount of physically and chemically adsorbed water for Aluspher AL100 may be less accurate than for other porous oxide samples.

As far as the mass-loss curve for LiChrospher Si-100 is concerned, the decrease in mass up to about 500 K corresponds to the thermodesorption of physically adsorbed water molecules, where nearly all water is removed when the temperature of approximately 400 K is attained. Between 500 and

700 K the mass of the silica is nearly constant. This is followed by a decrease in mass with a maximum rate at about 900 K corresponding to the condensation of surface silanols [7,8].

Shown in Table 1 are the estimated amounts of water physically and/or chemically adsorbed on the surfaces of porous inorganic oxides under study, where the S_{BET} values for the samples outgassed at 473 K (see Table 2) were used. As can be seen, the amount of surface-coordinated water per m^2 of the dry material is the smallest for LiChrospher Si-100 silica (about $10 \mu\text{mol}/\text{m}^2$). In comparison to the water contents for LiChrospher Si-100, the amounts of physisorbed/chemisorbed water are two times higher for the Titania 100A and Zirconia PICA-7, and three times higher for Aluspher AL100. Moreover, for the silica sample, mostly physically adsorbed water appears to be removed up to 623 K, but the titania, zirconia and alumina samples probably contain significant amounts of both physically adsorbed and chemisorbed water that can be removed in the same temperature range. The complexity of interactions of water molecules with surfaces of titania, zirconia and alumina indicate the rich surface chemistry of these materials compared to silica. Chromatographic properties of these materials were recently studied under normal- and reversed-phase conditions [12]. It was shown that neither the selectivity nor the elution order were affected by the degree of crystallinity. It appears that the specific surface area, the degree of the surface hydration and the surface acidity–basicity control the retention by native oxides under normal-phase conditions. In contrast to silica, the basic properties of alumina, titania and zirconia make them promising for separations of basic compounds [12]. However, their surface properties are not as well understood as those of silica [10], which is one of the reasons these inorganic oxides tend to be less popular in chromatographic applications than silica-based packings.

The low-pressure behavior (Fig. 3) and adsorption energy distributions (Fig. 4) for the inorganic oxides can be interpreted in terms of the exposure of high energy adsorption sites on the surfaces of these materials caused by the thermal treatment, and the changes in the nitrogen adsorption behavior are consistent with the mass-loss profiles for all oxides under study.

The isotherms for the silica sample treated at 413, 473 and 623 K are essentially the same (Fig. 3). Consequently, the AED functions (Fig. 4) are identical and indicate the presence of three main types of adsorption sites with adsorption energies of about 5, 8 and 13 kJ/mol. The fact that the adsorption behavior of the silica is not dependent on the outgassing temperature is consistent with its mass-loss profile (Fig. 5), as the mass is relatively constant between 400 and 600 K. It appears that outgassing the silica sample at 413 K is sufficient to remove most of the adsorbed water, and consequently no further changes in the adsorption behavior are noted for higher outgassing temperatures.

The adsorption isotherms for the Aluspher AL100 alumina outgassed at 393 and 473 K do not differ appreciably (Fig. 3). However, the sample treated at 623 K exhibits a significantly different adsorption profile. The adsorption energy distributions (Fig. 4) indicate at least three main types of adsorption sites for alumina with adsorption energies of about 5, 10 and 14 kJ/mol. The AED functions for samples outgassed at 393 and 473 are nearly the same, but after the treatment at 623 K, the height of the peak at about 10 kJ/mol decreased and the height of the 14 kJ/mol peak increased. Hence, the thermal treatment at 623 K increased the population of high adsorption energy sites, most likely due to desorption of water from them, which made them accessible for nitrogen adsorbate. Aluspher AL100 exhibits a continuous mass-loss profile up to 1200 K (Fig. 5). Moreover, the alumina was estimated to possess significant amounts of surface associated water (see Table 1). The adsorption measurements indicate that the thermal treatment up to 473 K removes large amounts of physically adsorbed and/or weakly chemisorbed water (i.e. not associated with high energy adsorption sites). The thermal treatment at much higher temperatures (e.g., 623 K) appears to remove a fraction of the more strongly chemisorbed water, thereby revealing high energy adsorption sites on the alumina surface.

The low-pressure adsorption for Zirconia PICA-7 increased for the sample treated at the temperatures in the range from 373 to 623 K (Fig. 3). The AED functions (Fig. 4) indicate that the zirconia sample possesses two main types of adsorption sites at approximately 6 and 15 kJ/mol. Some adsorption

sites with energy of about 10 kJ/mol may also be present. These may correspond to different types of hydroxyl groups or water chemisorbed at surface sites, but the assignment of peaks in the distribution to particular types of adsorption sites would be rather difficult. The slow and steady increase in the low-pressure adsorption for zirconia can be interpreted in terms of its mass-loss profile (Fig. 5). Zirconia PICA-7 contained an appreciable amount of surface-associated water (see Table 1). However, most of this water (about 1% of sample mass) was gradually removed up to 400 K. A much smaller mass-loss (approx. 0.2%) occurs between 400 and 600 K. The changes in the low-pressure adsorption and AED functions caused by the thermal treatment of zirconia are also gradual. It can be seen that the amount of sites of the highest adsorption energy (i.e. 15 kJ/mol) increases at the expense of the 10 kJ/mol sites, whereas the population of lowest energy sites (6 kJ/mol) remains essentially unchanged.

Among the porous oxides studied, the effects of the thermal treatment in the 373–623 K temperature range were most pronounced for Titania 100A. The changes in the adsorbed amount and the isotherm shape (Fig. 3) are the largest for the sample outgassed at 373 and 413 K. The AED function for titania reveals significant changes in the surface properties of the material. Following the thermal treatment at 373 K, the AED function for titania (Fig. 4) indicates three main types of adsorption sites with adsorption energies of about 5, 10 and 13 kJ/mol. After the treatment at 413 K, the population of 10 kJ/mol sites decreased significantly, whereas the amount of highest energy sites substantially increased. An even greater amount of high energy adsorption sites can be noticed after outgassing at temperatures from 473 to 623 K, for which two main types of adsorption sites with energies of about 5 and 13 kJ/mol are present in the distribution functions. As previously noted, two distinct types of residual hydroxyl groups have been reported for dry anatase on the basis of infrared measurements [34–36]. Similarly as for the other oxides, the mass-loss profile for titania provides insight into the changes in surface properties induced by the thermal treatment. The removal of adsorbed water for Titania 100A takes place in two distinct steps up to about 600 K (Fig. 5). Therefore, outgassing of the sample at

different temperatures in the range from 373 to 623 K enabled us to probe the surface of titania with significantly varying amounts of high energy adsorption sites.

4. Conclusions

A combination of thermogravimetry and nitrogen adsorption over a wide range of pressures allowed the gain of much insight into surface and structural properties of the chromatographic porous oxides studied. Adsorption data were used not only to calculate the specific surface areas and pore size distributions for the samples, but also to assess their surface properties, i.e. their interactions with nitrogen probe molecules. All the porous oxides under study have rather narrow mesopore size distributions, which is desirable for chromatographic purposes. The surface properties of titania, and to a smaller extent zirconia and alumina, were found to be dependent on the thermal treatment of the samples in the temperature range from 373 to 623 K. The increases in the population of high energy adsorption sites, observed from low-pressure adsorption data, were attributed to the exposure of these sites to the nitrogen adsorbate after the physically/chemically adsorbed water was removed by the thermal treatment. There appeared to be a good correlation between the changes in the low-pressure nitrogen adsorption isotherms and the shape of thermogravimetric mass-loss curves for all oxides studied. The current study shows that surface properties of porous oxides can be effectively probed by low-pressure nitrogen adsorption measurements. As was previously indicated [10], the detailed investigation of the surface and structural properties of porous materials facilitates their applications as chromatographic packings.

Acknowledgements

The authors thank Zirchrom Separations, E. Merck and YMC for providing the samples of zirconia, alumina and titania, respectively.

References

- [1] R.P.W. Scott, *Silica Gel and Bonded Phases*, Wiley, Chichester, 1993.
- [2] E.F. Vansant, P. Van Der Voort, K.C. Vrancken, *Characterization and Modification of the Silica Surface*, Elsevier, Amsterdam, 1995.
- [3] K.K. Unger (Ed.), *Packings and Stationary Phases in Chromatographic Techniques*, Marcel Dekker, New York, 1990.
- [4] J.J. Kirkland, J.W. Henderson, J.J. DeStefano, M.A. van Straten, H.A. Claessens, *J. Chromatogr. A* 762 (1997) 97.
- [5] K.K. Unger, N. Becker, P. Roumeliotis, *J. Chromatogr.* 125 (1976) 115.
- [6] Cs. Horváth, W. Melander, I. Molnár, *Anal. Chem.* 49 (1977) 142.
- [7] K.K. Unger, *Porous Silica (Journal of Chromatography Library, Vol. 16)*, Elsevier, Amsterdam, 1979.
- [8] R.K. Iler, *The Chemistry of Silica*, Wiley-Interscience, New York, 1979.
- [9] U. Trüding, G. Müller, K.K. Unger, *J. Chromatogr.* 535 (1990) 111.
- [10] J. Nawrocki, M.P. Rigney, A. McCormick, P.W. Carr, *J. Chromatogr. A* 657 (1993) 229.
- [11] J.J. Pesek, V.H. Tang, *Chromatographia* 39 (1994) 649.
- [12] A. Kurganov, U. Trüding, T. Isaeva, K.K. Unger, *Chromatographia* 42 (1996) 217.
- [13] D.A. Hanggi, N.R. Marks, *LC·GC* 11 (1993) 128.
- [14] M. Jaroniec, in: A. Dąbrowski, V.A. Tertykh (Eds.), *Adsorption on New and Modified Inorganic Sorbents*, Elsevier, Amsterdam, 1996, p. 411.
- [15] Y. Bereznitski, M. Jaroniec, M. Kruk, *J. Liq. Chromatogr.* 19 (1996) 1523.
- [16] Y. Bereznitski, M. Jaroniec, M. Kruk, B. Buszewski, *J. Liq. Chromatogr.* 19 (1996) 2767.
- [17] M. Kruk, M. Jaroniec, R.K. Gilpin, Y.W. Zhou, *Langmuir* 13 (1997) 545.
- [18] C.P. Jaroniec, R.K. Gilpin, M. Jaroniec, *J. Phys. Chem. B* 101 (1997) 6861.
- [19] S.J. Gregg, K.S.W. Sing, *Adsorption, Surface Area and Porosity*, Academic Press, London, 1982.
- [20] M. Jaroniec, R. Madey, *Physical Adsorption on Heterogeneous Solids*, Elsevier, Amsterdam, 1988.
- [21] J. Köhler, D.B. Chase, R.D. Farlee, A.J. Vega, J.J. Kirkland, *J. Chromatogr.* 352 (1986) 275.
- [22] P. Staszczuk, M. Jaroniec, R.K. Gilpin, *Thermochim. Acta* 287 (1996) 225.
- [23] T. Czajkowska, M. Jaroniec, B. Buszewski, *J. Chromatogr. A* 728 (1996) 213.
- [24] Y.W. Zhou, M. Jaroniec, R.K. Gilpin, *J. Colloid Interface Sci.* 185 (1997) 39.
- [25] P. Staszczuk, M. Jaroniec, R.K. Gilpin, in: J. Keller, E. Robens (Eds.), *Microbalance Techniques*, Multi-Science Publ. Co., Brentwood, 1994, p. 101.
- [26] J. Nawrocki, P.W. Carr, M.J. Annen, S. Froelicher, *Anal. Chim. Acta* 327 (1996) 261.
- [27] S. Brunauer, P.H. Emmett, E. Teller, *J. Am. Chem. Soc.* 60 (1938) 309.
- [28] E.P. Barrett, L.G. Joyner, P.P. Halenda, *J. Am. Chem. Soc.* 73 (1951) 373.
- [29] C. Lastoskie, K.E. Gubbins, N. Quirke, *J. Phys. Chem.* 97 (1993) 4786.
- [30] K.S.W. Sing, D.H. Everett, R.A.W. Haul, L. Moscou, R.A. Pierotti, J. Rouquerol, T. Siemieniowska, *Pure Appl. Chem.* 57 (1985) 603.
- [31] J. Rouquerol, D. Avnir, C.W. Fairbridge, D.H. Everett, J.H. Haynes, N. Pernicone, J.D.F. Ramsay, K.S.W. Sing, K.K. Unger, *Pure Appl. Chem.* 66 (1994) 1739.
- [32] A. Clark, *The Theory of Adsorption and Catalysis*, Academic Press, New York, 1970.
- [33] M. von Szombathely, P. Brauer, M. Jaroniec, *J. Comput. Chem.* 13 (1992) 17.
- [34] M. Primet, P. Pichat, M.V. Mathieu, *J. Phys. Chem.* 75 (1971) 1216.
- [35] D.J.C. Yates, *J. Phys. Chem.* 65 (1967) 746.
- [36] K.I. Hadjiivanov, D.G. Klissurski, *Chem. Soc. Rev.* 0 (1996) 61.
- [37] V. Bolis, C. Mortera, M. Volante, L. Orto, B. Fubini, *Langmuir* 6 (1990) 695.
- [38] E. Guglielminotti, *Langmuir* 6 (1990) 1455.
- [39] A.A. Tsyganenko, V.M. Filimonov, *Spectrosc. Lett.* 5 (1972) 477.
- [40] W. Hertl, *Langmuir* 5 (1989) 96.
- [41] A.A. Tsyganenko, P.P. Mardilovich, *J. Chem. Soc., Faraday Trans.* 92 (1996) 4843.